Rapid Poly(ethylene oxide) Segmental Dynamics in Blends with Poly(methyl methacrylate)

T. R. Lutz, Yiyong He, and M. D. Ediger*

Chemistry Department, University of Wisconsin—Madison, 1101 University Ave., Madison, Wisconsin 53706

Haihui Cao, Guoxing Lin, and Alan A. Jones*

Carlson School of Chemistry and Biochemistry, Clark University, Worchester, Massachusetts 01610

Received October 28, 2002; Revised Manuscript Received January 6, 2003

ABSTRACT: Miscible blends of perdeuteriopoly(ethylene oxide) (d_4PEO) and poly(methyl methacrylate) (PMMA) were studied using deuterium NMR over the concentration range of 0.5−30% d_4PEO using 2−4 Larmor frequencies ranging from 31 to 76 MHz. Spin−lattice relaxation times and line widths were measured from 300 to 475 K. Over this range PEO is liquidlike or rubbery in terms of its dynamics even though many of the measurements are below the blend glass transition temperature. There is no indication of the DSC glass transition in terms of a jump in either the spin−lattice relaxation times or the line widths. A model suitable for a rubber solid was used to interpret the spin−lattice relaxation times in terms of segmental motion and backbone libration. Segmental correlation times for d_4PEO fall in the nanosecond range with a very broad distribution of correlation times described by a KWW β of about 0.27. The segmental dynamics of d_4PEO are 12 orders of magnitude faster than PMMA segmental dynamics for a 3% d_4PEO blend near the blend T_g. Over the temperature range studied, d_4PEO segmental dynamics are nearly independent of composition for blends from 0.5% to 30% d_4PEO. At the lowest concentration studied, d_4PEO is in the dilute solution range; this eliminates intermolecular concentration fluctuations as an explanation of the rapid d_4PEO dynamics. These observations are unusual for miscible polymer blends and cannot be described by current models.

Introduction

Understanding and being able to accurately predict dynamics in miscible binary polymer blends is a critical precursor toward understanding dynamics in more complex multicomponent systems. Dynamics in miscible blends are challenging because the polymer chains are in intimate contact with each other. Each component is strongly influenced by the presence of the other. Polymer blends are also technologically important,[1] further motivating an increased understanding of their properties. While significant effort has been made toward the understanding of component dynamics in blends,[2−21] it is not yet possible to accurately predict dynamic properties of blends from information using only pure component data.

Dynamics of some binary miscible blend systems have been studied in detail, including polyisoprene/poly(vinylethylene) (PI/PVE),[2−5] polystyrene/poly(2,6-dimethylphenylene oxide) (PS/PXE),[6,7] polystyrene/poly(vinyl methyl ether) (PS/PVME), and poly(ethylene oxide)/poly(methyl methacrylate) (PEO/PMMA).[22−24] These studies focus on component dynamics in blends with intermediate compositions, 20−80%. While several models attempt to predict blend dynamics, none of these can accurately account for the dynamics observed in all four of these miscible blend systems. The variables affecting blend dynamics are thought to include intrinsic mobility differences between the chains, coupling between the chains, self-concentration effects, and composition fluctuations of the system.[17−21]

PEO/PMMA is a miscible blend system which has been the focus of several previous studies.[22−30] PEO/PMMA blends display a small negative interaction parameter χ, but the system is complicated by the presence of crystallization of PEO as the composition of PEO is increased above 20−30%.[27,28] There is a single DSC glass transition for the amorphous component of the blend indicating a true blend, but the small value of χ leads to large concentration fluctuations. Amorphous heterogeneities in the range 2−50 nm have been reported on the basis of NMR measurements.[29] Positron annihilation lifetime spectroscopy also indicates a bimodal distribution of "free volume" consistent with local heterogeneity.[30] Colby and co-workers[22] report that time−temperature superposition fails for this blend.[25,26] The large difference in glass transition temperatures between PEO and PMMA and their WLF parameters indicate widely differing time scales of motion for the two polymers before blending.[25,26] A ^{1}H NMR study of Cohen-Addad and co-workers[22] investigated the PEO dynamics in blends down to 20% PEO. These studies indicate that PEO segmental dynamics may be up to 9 orders of magnitude faster than PMMA segmental dynamics at the glass transition temperature T_g of the 20% PEO blend. This result indicates a larger segmental dynamics difference between d_4PEO and PMMA than has been observed in other miscible blends.

In this contribution, ^{2}H NMR was used to study a blend of deuterated poly(ethylene oxide) with poly(methyl methacrylate) for concentrations ranging from 0.5% to 30% d_4PEO. For each composition we performed ^{2}H NMR T_1 measurements from 300 to 475 K at 2−4 different magnetic fields. To obtain a quantitative description of segmental motion, correlation times were extracted using a modified Kohlrausch−Williams−Watts (mKWW) correlation function coupled with a Vogel−Tamman−Fulcher (VTF) temperature dependence. Since ^{2}H NMR data have a more direct inter-

10.1021/ma021634o CCC: $25.00
Published on Web 02/04/2003

pretation than that of ^{1}H NMR, an improved description of segmental motion is anticipated. In addition, this study of d_4PEO dynamics extends into the "infinite" dilution regime. This infinite dilution approach is not only different from the previous studies of PEO/PMMA but has also not been taken for any other polymer blend system. In the limit of infinite dilution, intermolecular composition fluctuations are unimportant. By removing these composition fluctuations, the problem is simplified, allowing for the investigation of intrinsic mobility difference and self-concentration effects on polymer dynamics.

There are two major findings in this study of d_4PEO/PMMA blend dynamics. First, at the blend T_g, d_4PEO segmental dynamics are found to be 12 orders of magnitude faster than PMMA segmental dynamics for a 3% d_4PEO blend. Second, over the temperature range studied, d_4PEO segmental dynamics are nearly independent of composition for blends containing 0.5−30% d_4PEO. These characteristics are unusual for miscible polymer blends and cannot be predicted by current models. We present a physical picture that would account for the extreme behavior of this system. We propose that because d_4PEO lacks side groups, segmental motion remains extremely fast, allowing the d_4PEO chain to locally relax in a "solid" matrix formed by glassy PMMA.

Experimental Section

Materials. Deuterated poly(ethylene oxide-d_4) terminated at one end by −OH and at the other end by $-OCH_3$ was purchased from Polymer Source (#P2362-dEO). The d_4PEO has $M_w = 1.25 \times 10^5$ g/mol with a polydispersity index of 1.07. Poly(methyl methacrylate), $M_w = 1.06 \times 10^5$ g/mol, PI = 1.16, was also purchased from Polymer Source (#P1398-MMA). The PMMA was greater than 79% syndiotactic. Additionally, a 20% blend sample was kindly provided by Professor Ralph Colby; it was prepared using d_4PEO with $M_w = 1.22 \times 10^5$ g/mol and PMMA with $M_w = 5.49 \times 10^5$ g/mol.

Blend Preparation. Four d_4PEO/PMMA blends of 0.5, 3, 6, and 20% d_4PEO were prepared via freeze-drying with HPLC grade benzene for ^{2}H NMR measurements taken at 46 and 76 MHz. The 10, 20, and 30% d_4PEO blends were prepared by solvent-casting from benzene solution for NMR measurements at 32 and 64 MHz. One 20% d_4PEO sample was cast from acetone. All compositions specified in this paper are mass percent.

For freeze-drying, up to 1 g of mixed polymers was dissolved in ∼25 mL of benzene. The sample was filtered using a 0.2 μm filter and introduced dropwise to a round-bottom flask which was precooled in liquid nitrogen. The sample was then monitored closely to ensure a heating rate under vacuum of approximately 5 K/h from 243 to 273 K. The sample was heated for 2 h at 350 K to ensure complete removal of solvent. The blend was then transferred to NMR tubes, sealed under vacuum, and stored at 273 K until NMR measurements were performed.

The cast samples were prepared by mixing dilute solutions of the component polymers and then stripping the solvent at room temperature using a vacuum. Vacuum drying was continued either for days at room temperature or for hours at 400 K to ensure removal of all solvent.

T_g and Miscibility. Differential scanning calorimetry thermograms were obtained using a Seiko SSC 220C DSC calibrated to a heating rate of 10 K/min using melting points of indium and gallium. Samples were hermetically sealed in 15 μL Seiko aluminum DSC pans. Previous studies indicate miscibility for blends of less than 20−30% PEO.[25] DSC thermograms of our samples indicate blend miscibility by the presence of a single T_g. In addition, there was no evidence in our NMR measurements indicating blend immiscibility. The line width of the 20% d_4PEO blend is greater than 10 times that of the line width of pure d_4PEO at 325 K. If PEO-rich regions were present in the blend, we would expect to see a peak with line width comparable to that of pure d_4PEO superimposed on a broader base. This was not observed and, while not a rigorous test of blend miscibility, does corroborate the DSC results. Table 1 provides a summary of the DSC characterization of the d_4PEO/PMMA blends.

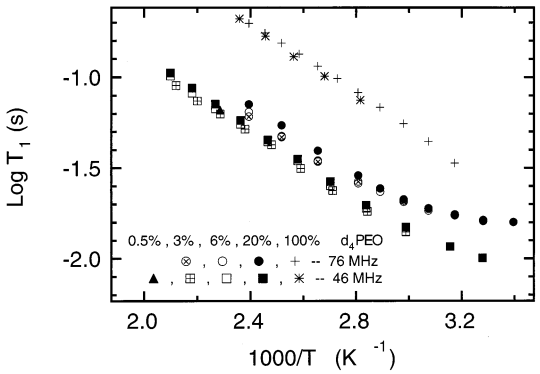

Figure 1. ^{2}H NMR relaxation time measurements for deuterated poly(ethylene oxide) at 46 and 76 MHz for d_4PEO/PMMA blends containing 0.5, 3, 6, and 20% d_4PEO as well as pure d_4PEO.

Table 1. Blend Characterization

wt % d_4PEO	DSC T_g(K)
0	405
3	391
6	383
20	356

NMR Measurements. Spin−lattice relaxation measurements T_1 were performed using ^{2}H NMR and the standard inversion recovery ($\pi-\tau-\pi/2$) pulse sequence. T_1 measurements induce inversion of the macroscopic magnetization and then measure the time for the magnetization to return to its equilibrium state.

^{2}H NMR measurements were performed at four frequencies using four different NMR spectrometers: Varian Inova-500 NMR spectrometer (76.7 MHz),Varian Inova Wide Bore-400 NMR (62 MHz), Bruker DMX-300 NMR (46.1 MHz), and Varian Mercury-200 NMR (31 MHz). Temperature was controlled to ±0.5 K and calibrated to an uncertainty of ±2 K using an ethylene glycol thermometer, melting point standards, or both. Data were processed with line broadening equal to one-tenth the line width of the spectra, and the magnetization relaxation was fit with three parameters to obtain T_1. Peak intensity and peak area were both employed and yielded T_1 values that agreed to within the experimental error of our measurements (5%). For the more dilute samples, a minimum of four trials were averaged to obtain T_1. At higher concentrations of d_4PEO, only one or two determinations of T_1 were made.

Results

Figures 1 and 2 show measured ^{2}H T_1 values for d_4-PEO in the various d_4PEO/PMMA blends. Figure 1 shows the ^{2}H T_1 values for 0.5, 3, 6, and 20% d_4PEO as well as pure d_4PEO taken at the ^{2}H Larmor frequencies 46 and 76 MHz. Figure 2 contains ^{2}H T_1 values for 10, 20, and 30% d_4PEO taken at 32 and 64 MHz ^{2}H Larmor frequencies. The data in Figure 2 are for films cast from benzene; the 20% sample cast from acetone provided by Professor Ralph Colby gave the same results within experimental error. There is no indication that the method of sample preparation had any influence on the measured T_1 values.

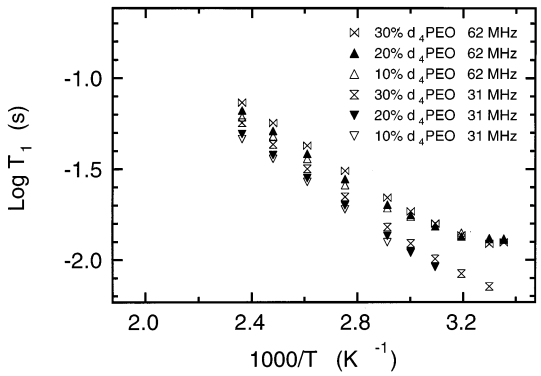

Figure 2. ^{2}H NMR relaxation time measurements for deuterated poly(ethylene oxide) at 31 and 62 MHz for d_4PEO/PMMA blends containing 10, 20, and 30% d_4PEO.

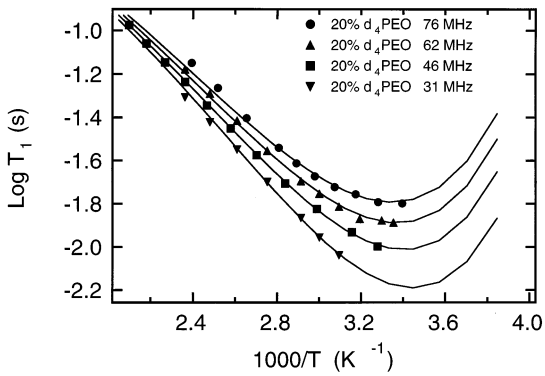

Figure 3. Simultaneous fit to 20% d_4PEO measurements at 31, 46, 62, and 76 MHz. Equations 1−6 were employed to obtain this fit. B was constrained to 354 K and a_{lib} to 0.1. β, T_0, and τ_∞ in eqs 4 and 5 were then freely adjusted to obtain the best fit to the experimental data. Best fit parameters are presented in Table 2.

Data Interpretation

NMR Relaxation Equations. Relaxation of the ^{2}H nuclear spin is dominated by electric quadrupole coupling of deuterium nuclei. As shown below, the relaxation of the deuterium nuclei is related to the reorientation of the C−D bond.[31,32] The spin−lattice relaxation time of deuterium can be written as

$$\frac{1}{T_1} = \frac{3}{10}\pi^2\left(\frac{e^2qQ}{h}\right)^2 [J(\omega_D) + 4J(2\omega_D)] \qquad (1)$$

Here $\omega_D/2\pi$ is the Larmor frequency. The quadrupole coupling constant e^2qQ/h was taken as 155 ± 3 kHz (determined from the solid-state echo line shape at −90 °C) for d_4PEO deuterons. In eq 1, $J(\omega)$ is the spectral density function, and is the Fourier transform of the orientation autocorrelation function $G(t)$, for the C−D bond:

$$J(\omega) = \frac{1}{2}\int_{-\infty}^{\infty} G(t)e^{-i\omega t}\,dt \qquad (2)$$

$G(t)$ is the function of our interest and can be written as

$$G(t) = \frac{3}{2}\langle\cos^2\theta(t)\rangle - \frac{1}{2} \qquad (3)$$

where $\theta(t)$ is the angle of the C−D bond relative to its orientation at time $t = 0$.

Correlation Function and Correlation Time. We assume a modified Kohlrausch−Williams−Watts (mKWW) functional form for the orientation autocorrelation function. This functional form has been previously employed and found to give excellent agreement with experimental data.[5,33,34]

$$G(t) = a_{lib}e^{-t/\tau_{lib}} + (1 - a_{lib})e^{-(t/\tau_{seg})^\beta} \qquad (4)$$

This function indicates that C−D vector reorientation occurs via two mechanisms: librational and segmental motions. In this equation a_{lib} and τ_{lib} are the amplitude and relaxation time for librational motion; τ_{lib} is set to 1 ps in our fitting analysis as the fit is insensitive to this value. The remaining two parameters in this equation, τ_{seg} and β, describe a characteristic segmental relaxation time as well as the distribution of times associated with it. We assume that τ_{seg} has a Vogel−Tamman−Fulcher (VTF) temperature dependence:

$$\log\left(\frac{\tau_{seg}}{\tau_\infty}\right) = \frac{B}{T - T_0} \qquad (5)$$

where τ_∞, B, and T_0 are constants for a given component in a particular blend. The correlation time for segmental dynamics $\tau_{seg,c}$ is the time integral of the segmental portion of the correlation function:

$$\tau_{seg,c} = \frac{\tau_{seg}}{\beta}\Gamma\left(\frac{1}{\beta}\right) \qquad (6)$$

Fitting to mKWW and VTF Functions. Fitting of the deuterium T_1 data was performed for each blend using eqs 1−6. Blends for each composition were fit simultaneously for all fields in which they were studied. In this fitting procedure there are five unknown parameters: a_{lib}, τ_∞, β, B, and T_0. Because of the relatively small range of correlation times sampled in these measurements, B and T_0 are highly correlated with each other. Based on preliminary fits, B was constrained to be 354 K for all blends studied. In addition, the amplitude of libration was assumed to be unchanged by the environment of the d_4PEO chains, and consequently a_{lib} was constrained to a value of 0.1 for each blend. Figure 3 shows data for the 20% d_4PEO blend at four fields together with the fit obtained from the data set. The fit is excellent.

Parameters for all fits are given in Table 2. The small β values indicate a very broad distribution of relaxation times for d_4PEO. The values of β for d_4PEO is these blends are much smaller than observed for components in other miscible blend systems. At present, the reason for these differences are not apparent. T_0 decreases monotonically with increasing d_4PEO concentration except for that of the 10% blend. This minor irregularity is not a surprise since an error of 2−3 K is reasonable for T_0 in these fits given that the data cover a narrow frequency range and do not reach the T_1 minimum. Pure d_4PEO was fit in the same manner as the blend data. An array of fitting parameters provided comparable fits. Consequently, while the correlation times calculated for pure d_4PEO are considered accurate, the parameter values for pure d_4PEO in Table 2 should be considered with caution.

Table 2. Fit Parameters for d_4PEO Dynamics in Blends[a]

	3% d_4PEO	6% d_4PEO	10% d_4PEO	20% d_4PEO	30% d_4PEO	pure d_4PEO
β	0.27	0.27	0.27	0.28	0.28	0.33
τ_∞ (ps)	0.12	0.11	0.11	0.12	0.10	0.10
T_0 (K)	212	211	212	207	202	166
fields fit (MHz)	46, 76	46, 76	32, 64	32, 46, 64, 76	32, 64	46, 76

[a] Fits to eqs 4 and 5; for all fits $a_{lib} = 0.1$ and $B = 354$ K.

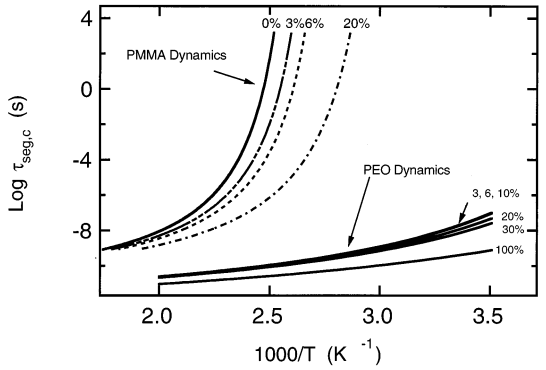

Figure 4. Segmental correlation times for both components in d_4PEO/PMMA blends at various compositions. Solid lines for d_4PEO are the result of fits of experimental data to the mKWW function with a VTF temperature dependence. Pure PMMA (labeled 0% meaning 0% d_4PEO is present) dynamics are the VTF fit from dielectric relaxation measurements of Bergman et al. PMMA dynamics in blends containing 3, 6, and 20% d_4PEO were predicted assuming PMMA dynamics are reflective of the blend T_g and that PMMA maintains a VTF temperature dependence in the blends. A 12 order of magnitude segmental dynamic difference exists between PEO and PMMA segmental dynamics at the blend T_g for a 3% blend. PEO has a very weak composition dependence over the temperature regime studied.

Correlation Times. After fitting the T_1 data as described above, we calculate the segmental correlation time $\tau_{seg,c}$ of d_4PEO in the various blends (eq 6). Figure 4 presents the segmental correlation times of pure d_4-PEO as well as for d_4PEO in the blends. An error bar of ± 0.25 decades is associated with the segmental correlation time for d_4PEO at the lowest temperatures; this diminishes to ± 0.1 decades at the highest temperatures studied for all compositions.

The T_1 minimum was not reached in these experiments because the deuterium line widths for d_4PEO get very broad as the temperature decreases. The data presented are the T_1 values for which the fwhm line width is less than 18 000 Hz. A transition from a liquid view to a solid-state view is required to interpret the data past this regime where a solidlike quadrupolar pattern begins to emerge. A different interpretational approach from eqs 1−6 would be required. A study of dynamics via quadrupolar echo line shapes is being made at lower temperatures and will be reported later.

Discussion

PMMA Dynamics in d_4PEO/PMMA Blends. In this study, dynamic information was measured only for d_4PEO in the d_4PEO/PMMA blends. To allow a comparison between the dynamics of both components, the segmental dynamics of PMMA measured by Bergman et al.[35] were used to predict the dynamics of PMMA in the various blends. These predictions are shown in Figure 4. The prediction for PMMA dynamics in the blends assumes PMMA dynamics maintain a VTF temperature dependence in the blend. PMMA dynamics were predicted using $T_0 = T_{g,blend} - 33$ K, where $T_{g,blend}$ is measured by DSC, and holding τ_∞ and B constant. This assumption is consistent with studies that indicate that the effective T_g for the slow component in the blend is nearly the blend T_g.[3−5] Any error associated with this assumption will be negligible in the limit of low PEO concentration.

d_4 PEO Dynamics in d_4PEO/PMMA Blends. Figure 4 shows d_4PEO segmental correlation times obtained by fitting T_1 data to eqs 1−6. Two significant and unusual features are found in Figure 4. First, d_4PEO segmental correlation times for blends of up to 30% d_4-PEO are nearly identical. Second, in the 3% d_4PEO blend, d_4PEO segmental dynamics are 12 orders of magnitude faster than the PMMA segmental dynamics at the blend T_g. This magnitude of decoupling of the segmental dynamics of the two components in a miscible polymer blend has not previously been reported.

By investigating d_4PEO/PMMA blends in the dilute regime, the variables affecting dynamic properties have been simplified. For example, in a 20% or 30% d_4PEO/PMMA blend, the large difference between the segmental dynamics of the two components might have been ascribed to the presence of d_4PEO-rich domains. However, in the dilute limit, composition fluctuations are eliminated, and each d_4PEO chain is isolated and surrounded by PMMA chains. The critical overlap concentration c^* for d_4PEO of this molecular weight is about 1.5%. Measurements on 0.5% d_4PEO indicate identical dynamics to that of 3, 6, and 10% d_4PEO; thus, the 3% results can be interpreted assuming each d_4PEO chain is completely surrounded by PMMA units. The only contributions to d_4PEO dynamics for this blend are then the intrinsic mobility difference between the chains and self-concentration effects. Despite eliminating the possibility of d_4PEO-rich domains which might have accounted for fast dynamics, d_4PEO segmental dynamics remain on the nanosecond time scale when PMMA segmental dynamics slow to 100 s at the blend T_g. This combined with the weak composition dependence suggests that the segmental motions of a d_4PEO chain are decoupled from the PMMA matrix which surrounds it.

Our 20% d_4PEO results are in qualitative agreement with the ^{1}H NMR results of Cohen-Addad et al.[22] At the highest temperatures studied our correlation times are 1 decade slower than those reported by Cohen-Addad, and at the lowest temperatures this difference becomes less than half a decade. The ^{2}H NMR measurements reported here provide information about carbon−deuterium vector reorientation. In ^{1}H NMR, the relaxation of magnetization not only is due to H−H reorientation of hydrogens attached to the same carbon but also is a result of interactions with other nearby protons. These additional protons may be attached to other parts of the repeat unit or on other repeat units either on the same chain or neighboring chains. Presumably these additional interactions are responsible for the different segmental correlation times reported here and those reported from ^{1}H NMR.[22]

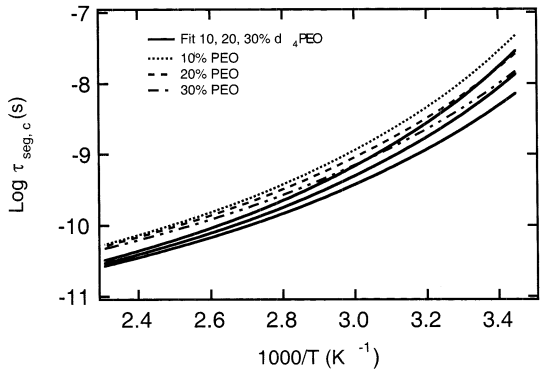

Figure 5. Lodge−McLeish fit of d_4PEO segmental correlation times for d_4PEO/PMMA blends of 10, 20, and 30% d_4PEO. One parameter, ϕ_{self}, was varied in the fitting; the best fit was obtained with $\phi_{self} = 0.57$. The blend T_g was predicted using the Fox equation.

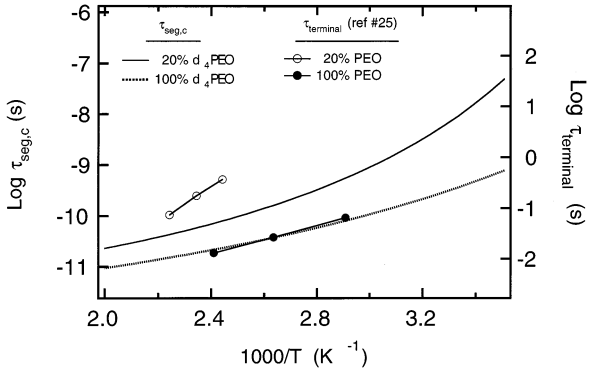

Figure 6. Comparison of segmental and terminal relaxation times for PEO in purePEO and in a 20% PEO blend. The right axis corresponds to terminal dynamics (lines with circles). Segmental correlation times resulting from fitting are plotted on the left axis (lines with no symbols). The ratio of τ_{term}/τ_{seg} for the melt is constant while for a 20% PEO blend this ratio has a temperature dependence.

A number of models have been introduced to predict dynamics of polymers in blends.[17−21] Figure 5 shows our attempt to fit the d_4PEO data with the model of Lodge and McLeish.[21] The model assumes a cooperative volume centered on a monomer of the polymer of interest. Within this cooperative volume the concentration of the polymer is enhanced over the bulk concentration due to chain connectivity. The relevant length scale is assumed to be the Kuhn length of the polymer in this model. We used the model of Lodge and McLeish not to predict segmental dynamics but to fit our data. The best fit was obtained by varying the self-concentration ϕ_{self} utilizing the VTF parameters for pure d_4PEO and assuming a Fox relationship for the blend T_g. The fitted value of ϕ_{self} for d_4PEO/PMMA is 0.57. While the Lodge and McLeish approach provides a reasonable fit to the data, the value of ϕ_{self} predicted by their approach is 0.15. We are not aware of any model that can predict the data.

Potential Artifacts. There are two potential artifacts that need to be addressed in the determination of the d_4PEO segmental dynamics.

As the distribution of relaxation times is very broad, could we have made a significant error in the correlation times as a result? The stretched exponential parameter β of the mKWW function is a measure of the distribution of relaxation times. In this study, a β of around 0.27 was found for each composition, signifying a very broad distribution (full width at half-maximum of 4−5 decades) of relaxation times for d_4PEO dynamics. With such a broad distribution present, it is useful to have an additional check on the extracted correlation times. This can be done for the NMR measurements taken here utilizing the fact that $T_2 \ll T_1$, where T_2 is the spin−spin relaxation time. An upper bound for segmental dynamics of d_4PEO in d_4PEO/PMMA blends can be calculated using T_2 which can be estimated from the observed line width. This upper bound is parallel to, but 3 orders of magnitude slower than, the segmental correlation times reported here. This upper bound does not necessarily indicate an error in the segmental correlation times. Rather, because T_2 relaxation contains low-frequency contributions (terminal relaxation) which are not present in T_1, this upper bound is expected to be considerably larger than the segmental correlation time. A large and significant dynamic difference between d_4PEO and PMMA of over 8 orders of magnitude would still exist at T_g in a 3% d_4PEO blend even if d_4PEO segmental correlation times were taken as the upper bound. This indicates that the dynamics of d_4PEO found by NMR are unequivocally many orders of magnitude faster than the PMMA dynamics at the blend T_g.

Have we really measured the segmental relaxation times (i.e., the α relaxation) for d_4PEO in the blends or are we reporting some faster motion? A comparison between the activation energy for pure d_4PEO extracted from NMR data to that of viscosity experiments shows that the dynamics reported here are consistent with an α relaxation. A viscosity study of PEO found the activation energy to be 6.4 kcal/mol.[36] The activation energy from our work is in good agreement at 6.5 kcal/mol. Also in good agreement with our NMR results is an apparent activation energy extracted from a ^{13}C NMR study[37] of 6.7 kcal/mol. This consistency argues strongly that what we report here is an α relaxation corresponding to segmental motion of PEO.

Comparison with Terminal Relaxation Dynamics. Figure 6 compares the temperature dependence of the terminal relaxation time of PEO as found by Colby[25,26] to its segmental dynamics both in the pure state and for a 20% PEO blend. While the temperature dependence of segmental and terminal dynamics are the same for pure d_4PEO, the temperature dependence of terminal dynamics in the 20% blend is much stronger than that of segmental dynamics. This means that the ratio of τ_{term}/τ_{seg} is not constant in the blend as is sometimes assumed in models of blend dynamics.[21] A changing ratio of τ_{term}/τ_{seg} is also consistent with the physical model for dynamics in d_4PEO/PMMA blends which we present below.

Comparison with Other Blends. None of the previously studied miscible blends display the extreme characteristics observed for the blend of d_4PEO/PMMA. Here we make a comparison with three miscible blend systems: polyisoprene/poly(vinyl ethylene) (PI/PVE), polystyrene/poly(2,6-dimethylphenylene oxide) (PS/PXE), and polystyrene/poly(vinyl methyl ether) (PS/PVME). PI/PVE studies[2−5] find an intrinsic mobility difference between the two polymer chains of a factor of 6 and segmental dynamics which differ by 2−5 orders of magnitude near the blend T_g. PS/PXE studies[6,7] find nearly identical segmental dynamics for each component at T_g, whereas in PS/PVME, segmental dynamic differences of 3−4 orders of magnitude are observed at the

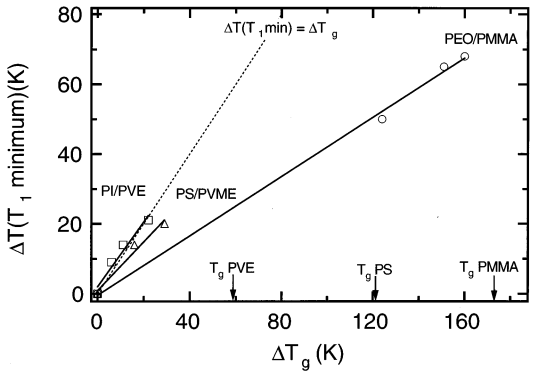

Figure 7. Decoupling of fast component segmental dynamics from the glass transition in three miscible polymer blend systems. The ordinate is the shift in temperature associated with ns segmental dynamics (T_1 minimum) for the fast component in the blend relative to its T_1 minimum in the homopolymer melt. The abscissa is the shift in the measured blend T_g relative to the homopolymer T_g for the fast component. A slope of 1 means that the segmental dynamics of the fast component are completely coupled with the blend T_g. This comparison is made for the fast component in three miscible polymer blend systems: PI/PVE, PS/PVME, and PEO/PMMA. PEO segmental dynamics are significantly decoupled from the blend T_g, as evidenced by the slope of 0.4, while PI segmental dynamics are intimately coupled to the blend T_g (slope of 1).

Table 3. Comparison of Miscible Polymer Blends

polymer blends	ΔT_g homopolymers (K)	$\tau_{seg,slow}/\tau_{seg,fast}$ at blend T_g	composition range
PS/PXE	115	$1-10^1$	25% PS
PI/PVE	60	10^2-10^5	25−75% PI
PVME/PS	120	10^3-10^4	50−65% PVME
PEO/PMMA	180	$10^{11}-10^{12}$	0.5−30% PEO

blend T_g.[8] Table 3 presents a compilation of results on these four miscible blends.

Another way of comparing these miscible polymer blends is to plot how the dynamics of the fast component shifts with the DSC T_g for the blend. Figure 7 presents the shift in the temperature of the T_1 minimum for the fast component against the shift in the blend T_g; both of these shifts are relative to the values for the pure fast component. Segmental dynamics at the T_1 minimum in NMR data are approximately 1 ns; thus, the ordinate shows the temperature shift associated with nanosecond dynamics of the fast component. Figure 7 compares the fast component in three miscible polymer blends: PI/PVE, PS/PVME, and PEO/PMMA. PI dynamics in PI/PVE blends changes nearly identically with the blend T_g, whereas d_4PEO dynamics in d_4PEO/PMMA are significantly decoupled from the glass transition of the blend. The fast components in these miscible blends have very different relationships with the glass transition of the blend.

Why Are d_4PEO Segmental Dynamics So Fast? High molecular weight, miscible blends of d_4PEO/PMMA have surprisingly fast PEO segmental dynamics. We propose here a physical picture that qualitatively explains these fast dynamics and their weak composition dependence.

An average PMMA segment at the glass transition of these blends is static on the time scale of PEO segmental motion. While PMMA segments immediately adjacent to PEO segments might show somewhat faster dynamics than other PMMA segments, as there is no experimental evidence for an extremely rapid PMMA component near the blend T_g, it is reasonable to assume that even these adjacent PMMA segments are fixed on the time scale of PEO motion. How is it possible that PEO chains can locally relax while directly adjacent PMMA chains are essentially frozen? We imagine that the lack of side groups on PEO is a key feature. The absence of a side group may allow nearly complete conformational relaxation of PEO without requiring any conformational rearrangement of nearby PMMA segments. This would explain both the large difference between segmental dynamics of the two components and the weak composition dependence of PEO segmental dynamics. This would also explain why the terminal relaxation time of PEO chains in the blends has a stronger temperature dependence than the segmental relaxation. Terminal relaxation requires that the end-to-end vector of the chain can rearrange; local conformational changes inside a rigid cage of PMMA would not allow global chain relaxation.

This physical model would suggest that another polymer with a larger side group, but with identical χ and chain length as the d_4PEO used here, would have segmental dynamics similar to what is observed in other miscible polymer blend systems. If this physical picture is correct, a larger side group would result in steric hindrance and the inability for such a polymer to locally relax at the fast rate observed for d_4PEO. This picture attributes the observations to characteristics of d_4PEO and assumes that the PMMA acts "normal". There is no evidence that PMMA acts differently from what would be expected, however, to completely eliminate PMMA as the answer; further studies on d_4PEO blend systems are required.

Conclusion

We have investigated the segmental dynamics of d_4-PEO in blends with PMMA utilizing ^{2}H NMR at four magnetic fields. The studies extended from the dilute regime up to 30% d_4PEO. The orientation autocorrelation function for C−D vectors in d_4PEO is well described by a modified Kohlrausch−Williams−Watts function. The mKWW function coupled with a VTF temperature dependence was employed to extract segmental correlation times. These correlation times in a blend containing 3% d_4PEO were found to be 12 orders of magnitude faster than the PMMA segmental dynamics at the blend T_g. Furthermore, the segmental dynamics of d_4PEO are nearly composition independent for blends containing 0.5−30% d_4PEO. These results for d_4PEO/PMMA are unusual in comparison to other miscible polymer blends. We have proposed a physical interpretation for the dynamics observed in this d_4PEO/PMMA blend in which the lack of side groups on the d_4PEO backbone allows for the observed behavior.

The different dynamic features found in miscible polymer blends present a problem for current models. To simplify the problem, we have extended blend studies into the "infinite" dilution regime. Intermolecular composition fluctuations are removed in this limit. Further studies of other blend systems in the dilute regime will enable a better understanding of the variables affecting polymer blend dynamics.

Acknowledgment. We thank XiaoHua Qiu for performing preliminary measurements. This research was supported by the National Science Foundation through the Division of Material Research, Polymer Program (DMR-0099849 and DMR-0209614). Measure-

ments were performed at the Instrument Center of the Department of Chemistry, University of Wisconsin—Madison, supported by NSF CHE-9508244 and CHE-9629688 and at the Carlson School of Chemistry and Biochemistry at Clark University supported by CHE-9808023. We thank Charles Fry and Marvin Kontney for their support and Heidi Mansour for help with DSC measurements.

Supporting Information Available: Representative ^{2}H NMR spectra at 76 MHz for d_4PEO in a 6% d_4PEO/PMMA blend. This material is available free of charge via the Internet at http://pubs.acs.org.

Note Added after ASAP Posting

This article was released ASAP on 2/4/2003 with an error in Table 2, column 6, row 2; the correct value is 0.10. The correct version was posted on 2/11/2003.

References and Notes

(1) Newman, S.; Paul, D. R. *Polymer Blends*; Academic Press: New York, 1978.
(2) Chung, G. C.; Kornfield, J. A.; Smith, S. D. *Macromolecules* **1994**, *27*, 964−973.
(3) Chung, G. C.; Kornfield, J. A.; Smith, S. D. *Macromolecules* **1994**, *27*, 5729−5741.
(4) Saxena, S.; Cizmeciyan, D.; Kornfield, J. A. *Solid State Nucl. Magn. Reson.* **1998**, *12*, 165−181.
(5) Min, B. C.; Qiu, X. H.; Ediger, M. D.; Pitsikalis, M.; Hadjichristidis, N. *Macromolecules* **2001**, *34*, 4466−4475.
(6) Chin, Y. H.; Zhang, C.; Wang, P.; Inglefield, P. T.; Jones, A. A.; Kambour, R. P.; Bendler, J. T.; White, D. M. *Macromolecules* **1992**, *25*, 3031−3038.
(7) Chin, Y. H.; Inglefield, P. T.; Jones, A. A. *Macromolecules* **1993**, *26*, 5372−5378.
(8) Cendoya, I.; Alegria, A.; Alberdi, J. M.; Colmenero, J.; Grimm, H.; Richter, D.; Frick, B. *Macromolecules* **1999**, *32*, 4065−4078.
(9) Green, P. F.; Kramer, E. J. *Macromolecules* **1986**, *19*, 1108−1114.
(10) Green, P. F.; Adolf, D. B.; Gilliom, L. R. *Macromolecules* **1991**, *24*, 3377−3382.
(11) Green, P. F. *J. Non-Cryst. Solids* **1994**, 815−822.
(12) Composto, R. J.; Kramer, E. J.; White, D. M. *Polymer* **1990**, *31*, 2320−2328.
(13) Composto, R. J.; Kramer, E. J.; White, D. M. *Macromolecules* **1992**, *25*, 4267−4174.
(14) Kim, E.; Kramer, E. J.; Wu, W. C.; Garrett, P. D. *Polymer* **1994**, *35*, 5706−5715.
(15) Kim, E.; Kramer, E. J.; Osby, J. O. *Macromolecules* **1995**, *28*, 1979−1989.
(16) Yang, X. P.; Halasa, A.; Hsu, W. L.; Wang, S. Q. *Macromolecules* **2001**, *34*, 8532−8540.
(17) Kumar, S. K.; Colby, R. H.; Kamath, S.; Pathak, J. A. Submitted to *J. Chem. Phys.*
(18) Kamath, S.; Colby, R. H.; Kumar, S. K.; Karatasos, K.; Floudas, G.; Fytas, G.; Roovers, J. E. L. *J. Chem. Phys.* **1999**, *111*, 6121−6128.
(19) McGrath, K. J.; Roland, C. M. *J. Non-Cryst. Solids* **1994**, *172*, 891−896.
(20) Kumar, S. K.; Colby, R. H.; Anastasiadis, S. H.; Fytas, G. *J. Chem. Phys.* **1996**, *105*, 3777−3788.
(21) Lodge, T. P.; McLeish, T. C. B. *Macromolecules* **2000**, *33*, 5278−5284.
(22) Lartigue, C.; Guillermo, A.; Cohen-Addad, J. P. *J. Polym. Sci., Polym. Phys.* **1997**, *35*, 1095−1105.
(23) Schantz, S. *Macromolecules* **1997**, *30*, 1419−1425.
(24) Dionisio, M.; Fernandes, A. C.; Mano, J. F.; Correia, N. T.; Sousa, R. C. *Macromolecules* **2000**, *33*, 1002−1011.
(25) Colby, R. H. *Polymer* **1989**, *30*, 1275−1278.
(26) Zawada, J. A.; Ylitalo, C. M.; Fuller, G. G.; Colby, R. H.; Long, T. E. *Macromolecules* **1992**, *25*, 2896−2902.
(27) Ito, H.; Russell, T. P.; Wignall, G. D. *Macromolecules* **1987**, *20*, 2213−2220.
(28) Hopkinson, I.; Kiff, F. T.; Richards, R. W.; King, S. M.; Farren, T. *Polymer* **1995**, *36*, 3523−3531.
(29) Schantz, S.; Veeman, W. S. *J. Polym. Sci., Polym. Phys.* **1997**, *35*, 2681−2688.
(30) Wastlund, C.; Maurer, F. H. J. *Macromolecules* **1997**, *30*, 5870−5876.
(31) Zhu, W.; Ediger, M. D. *Macromolecules* **1995**, *28*, 7549−7557.
(32) Bovey, F. A.; Mirau, P. A. *NMR of Polymer*; Academic Press: San Diego, 1996.
(33) Bandis, A.; Wen, W. Y.; Jones, E. B.; Kaskan, P.; Zhu, Y.; Jones, A. A.; Inglefield, P. T.; Bendler, J. T. *J. Polym. Sci., Polym. Phys.* **1994**, *32*, 1707−1717.
(34) Qiu, X. H.; Moe, N. E.; Ediger, M. D.; Fetters, L. J. *J Chem. Phys.* **2000**, *113*, 2918−2916.
(35) Bergman, R.; Alvarez, F.; Alegria, A.; Colmenero, J. *J. Non-Cryst. Solids* **1998**, *235*, 580−583.
(36) Maconnachie, A.; Vasudevan, P.; Allen, G. *Polymer* **1978**, *19*, 33−38.
(37) Dejean de la Batie, R.; Laupretre, F.; Monnerie, L. *Macromolecules* **1988**, *21*, 2052−2058.

MA021634O